

Development, in vitro, and in vivo assessments of PCL-gelatin- β TCP fibrous scaffolds for cardiac regeneration

Mahnaz Fathi¹, Nafiseh Baheiraei^{2*}, Nahid Moradi³, Majid Salehi^{4,5}, Sepehr Zamani⁶, Mehdi Razavi^{7,8,9}, Hossein Eyni^{10,11}

¹Department of Hematology, Faculty of Medical Sciences, Tarbiat Modares University, Tehran, Iran

²Tissue Engineering and Applied Cell Sciences Division, Department of Anatomical Sciences, Faculty of Medical Sciences, Tarbiat Modares University, Tehran, Iran

³Applied Cell Sciences Division, Department of Hematology, Faculty of Medical Sciences, Tarbiat Modares University, Tehran, Iran

⁴Tissue Engineering and Stem Cells Research Center, Shahrood University of Medical Sciences, Shahrood, Iran

⁵Regenerative medicine Research Center, Shahrood University of Medical Sciences, Shahrood, Iran

⁶Student Research Committee, School of Medicine, Shahrood University of Medical Sciences, Shahrood, Iran

⁷Bionix (Bionic Materials, Implants & Interfaces) Cluster, Department of Medicine, University of Central Florida College of Medicine, Orlando, Florida 32827, USA

⁸Department of Material Sciences and Engineering, University of Central Florida, Orlando, Florida 32816, USA

⁹Biomedical Engineering Program, Department of Mechanical and Aerospace Engineering, University of Central Florida, Orlando, Florida 32816, USA

¹⁰Student Research Committee, Iran University of Medical Sciences, Tehran, Iran

¹¹Department of Anatomy, Stem Cell and Regenerative Medicine Research Center, School of Medicine, Iran University of Medical Sciences, Tehran, Iran

Article Info



Article Type:
Original Article

Article History:
Received: 16 Mar. 2025
Revised: 23 May 2025
Accepted: 28 May 2025
ePublished: 17 Aug. 2025

Keywords:
 β TCP
PCL
Gelatin
Neovascularization
Electrospinning
Tissue engineering

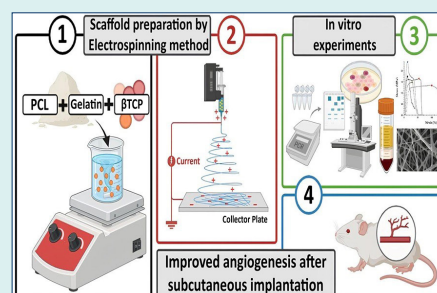
Abstract

Introduction: Cardiovascular disease is a leading cause of death worldwide. Tissue engineering offers a promising solution for promoting tissue regeneration at the infarcted site. In this study, beta-tricalcium phosphate (β TCP) was incorporated into poly(ϵ -caprolactone) (PCL) and gelatin (Gel) fibers for cardiac patch applications.

Methods: Electrospun scaffolds were prepared via electrospinning a 1:1 (w/w) mixture of PCL and Gel, embedding varying concentrations of β TCP at 0.25, 0.5, 1, and 3 wt.%. The scaffolds were analyzed through scanning electron microscopy (SEM), Fourier-transform infrared spectroscopy (FTIR), X-ray diffraction (XRD), tensile strength testing, hemolysis assays, toxicity testing, and quantitative reverse transcription polymerase chain reaction (qRT-PCR) for marker gene expression. Furthermore, subcutaneous scaffold implantation was performed to assess in vivo angiogenesis in NMRI mice. Tissue samples were examined using hematoxylin and eosin (H&E) staining and immunohistochemistry.

Results: According to the results, β TCP was uniformly distributed throughout the fiber scaffold, exhibiting a smooth, unbranched morphology with fiber diameters of approximately 75 μ m. Specifically, the mean diameters for PCL-Gel and PCL-Gel- β TCP at 3 wt.% were $45.01 \pm 2.82 \mu$ m and $100.91 \pm 11.69 \mu$ m, respectively. Mechanical property assessments revealed that the elastic modulus of the scaffolds was suitable for usage as a tissue-engineered cardiac patch. Scaffolds containing β TCP exhibited favorable blood compatibility and indicated no cytotoxicity at the tested concentrations. Furthermore, the expression levels of cardiac marker genes (Actn4, Connexin43, and TrpT2) were elevated in the treatment groups in conjunction with the escalation of β TCP dosage. Fiber composites with 1% β TCP were selected as the optimal scaffold for *in vivo* examination. This scaffold demonstrated a significantly enhanced cell migration rate, with a growth in capillary formation observed in the immunohistochemistry analysis.

Conclusion: The fibrous PCL-Gel- β TCP-1% scaffold showed optimal cell proliferation, blood compatibility and vascularization. These properties highlight its promise for cardiac tissue engineering.



*Corresponding author: Nafiseh Baheiraei, Email: n.baheiraei@modares.ac.ir



© 2025 The Author(s). This work is published by BioImpacts as an open access article distributed under the terms of the Creative Commons Attribution Non-Commercial License (<http://creativecommons.org/licenses/by-nc/4.0/>). Non-commercial uses of the work are permitted, provided the original work is properly cited.

Introduction

Over 17.9 million deaths occur worldwide annually owing to cardiovascular diseases (CVDs), making them the leading cause of global mortality. These conditions are expected to cause approximately 20 million deaths worldwide by 2030.¹ Myocardial infarction (MI) is a common CVD, resulting from an obstruction in blood flow. This blockage prevents the heart muscle from receiving adequate oxygen and nutrients, leading to the death of numerous cardiomyocytes (CMs) and the degradation of the extracellular matrix (ECM). This can ultimately result in life-threatening heart failure or sudden death.^{1, 2} Although there have been significant improvements in pharmacotherapy and surgery to restore heart function following a heart attack, it is still possible for the heart to regenerate itself completely, as adult heart muscle cells have limited ability to regenerate themselves. Accordingly, there is a great need for innovative approaches to delay the progression of myocardial damage.³⁻⁵

Tissue engineering is a promising branch of regenerative medicine integrating engineering principles, biology, and materials to offer viable solutions to replace, repair, or regenerate missing or damaged cells/tissues.⁶ Reconstruction of the heart's complex myocardial structure is an area where tissue engineering seeks to address its unfulfilled needs. By mimicking the shape and composition of the natural ECM, biomaterials such as injectable hydrogels or cardiac patches can be deployed at the site of MI to promote tissue regeneration and provide an effective method of treatment. Various biomaterial-based cardiac patches have been researched to enhance the mechanical function during heart attacks. The cardiac patch, a layered scaffold that can be surgically implanted onto the surface of the damaged myocardium, provides adequate space for cell adhesion, cell proliferation, ECM formation, and a variable rate of biodegradation based on the rate of the tissue regeneration. Meanwhile, they can serve as carriers capable of transporting bioactive cargoes such as bioactive molecules, drugs, cells, and exosomes, thus ameliorating the retention rate to achieve significant therapeutic effects.⁷⁻¹⁰

The electrospinning technique is employed to produce continuous nanofibers from solutions and is a simple synthetic process that can alter the fiber diameter from micrometers to nanometers.^{11,12} In addition, this technique allows manipulating significant factors such as the orientation and density of the fibers. Electrospun scaffolds present high levels of interconnectivity and porosity, making them suitable for temporary ECM functions. Not only do these nanofibers provide structural support to the cells but also exert a significant impact on the regulation of cellular activity.^{13,14}

Polycaprolactone (PCL), a synthetic polymer, is widely applied in the production of cardiac patches thanks to

its biocompatibility and gradual degradation, enabling long-lasting therapeutic effects in certain areas of tissue engineering.¹⁵⁻¹⁷ The U.S. FDA has approved for clinical use of PCL, making it a promising material with various applications in tissue engineering.¹⁸ The electrospun PCL nanofiber scaffold is similar in architectural structure to the ECM in living tissues, but its low hydrophilicity causes reduced ability for cell adhesion, migration, proliferation, and differentiation. To enhance the characteristics of the three-dimensional (3D) scaffold for cardiac tissue engineering, researchers have often used a combination of natural and synthetic polymers.¹⁷

Gelatin (Gel), a non-immunogenic and hydrophilic polymer derived from collagen through partial hydrolysis, is most widely used for fabricating cell-based scaffolds through tissue engineering. Gel has proved to be effective in combination with PCL.¹⁹⁻²² The incorporation of Gel to PCL has been shown to enhance the elastic modulus and structural stability of the scaffolds, making them suitable for usage as platforms for cardiac tissue modeling.²³⁻²⁷ Thanks to its biological properties and functional groups, Gel is a suitable substrate for facilitating cell adhesion, proliferation, and migration. Hybrid scaffolds have been developed by applying electrospinning techniques to combine PCL with Gel. According to studies, this combination holds promise as a scaffold for accelerating the regeneration of skeletal muscle,²⁸ bone,^{29,30} nerve,³¹ skin,³² periodontal,³³ cartilage,³⁴ tendon,³⁵ and cardiac.³⁶ In one study, electrospinning was employed to create random and aligned PCL-Gel composite nanofiber scaffolds that mimic the structure of the oriented ECM. When comparing PCL-Gel nanofiber scaffolds with electrospun PCL nanofibers, the results revealed that the former had lower stiffness, higher hydrophilicity, and smaller fiber diameters. Cardiomyocytes derived from rabbits were cultivated on randomly aligned electrospun nanofibers, in order to assess the biocompatibility and the ability of the scaffolds to guide cell behavior. Because of the biological components and ordered topography of the scaffolds, the aligned scaffold significantly improved cell adhesion and alignment, as presented by analyses using SEM and immunocytochemistry.³⁶ Gil-Castell and colleagues developed nanofibers using PCL/Gel/polyaniline (PANi) for cardiac tissue engineering. They altered the ratio of PCL to Gel and the dissolution time in the solvent before electrospinning to generate different samples. The inclusion of PANi was found to be non-toxic and resulted in a controlled increase in electrical conductivity, contributing to cardiomyocyte proliferation *in vitro*. The study found that the 40/60 PCL-Gel scaffold with 1.00 wt.% PANi indicated non-inflammatory properties and contributed to a reduction in scar tissue area once it was implanted into the rat heart 72 hours post-infarction.³⁵

When designing scaffolds for cardiac tissue engineering

and subsequent tissue regeneration, it is essential to ensure that the surface promotes bioactivity to facilitate cell adhesion, spreading, and proliferation. Literature indicates that calcium-based ceramics are valued in tissue engineering for their biodegradability and bioactivity, though their performance depends on physicochemical properties. Calcium sulfate resorbs rapidly *in vivo*, often before sufficient tissue forms, risking scaffold failure. Hydroxyapatite (HA) resorbs slowly, which can hinder tissue integration and stability.³⁷ β -tricalcium phosphate (β TCP) offers an intermediate degradation rate aligned with tissue regeneration timelines, making it advantageous. Additionally, β TCP releases calcium ions (Ca^{2+}), essential in tissue growth and angiogenesis, as endothelial Ca^{2+} signaling regulates endothelial cell proliferation, migration, and vasculogenesis. In cardiac tissue, Ca^{2+} is crucial for excitation-contraction coupling and gene regulation, underscoring β TCP's potential to support vascularization and myocardial regeneration via calcium release.³⁸⁻⁴⁰

Our aim in this research was to develop a new cardiac patch by mixing PCL and Gel (50:50) to resolve the weak mechanical strength and limited stability of the Gel, while improving the physicochemical properties and surface structure of the patch to promote cell infiltration and differentiation.¹⁹ β TCP is recognized for its exceptional biocompatibility and bioactivity, which are crucial for fostering cell adhesion, proliferation, and differentiation in tissue engineering applications.⁴¹ While predominantly employed in bone tissue engineering, these properties may also be beneficial for cardiac tissue by promoting cell integration and survival. The incorporation of β TCP into thin electrospun scaffolds, with caution regarding nanoparticle concentration, can potentially enhance their mechanical strength, a key attribute for sustaining the dynamic conditions present in the heart.⁴² The structural and mechanical properties of the final patch as well as the angiogenic properties of the nanofiber scaffolds were examined through *in vitro* research and subcutaneous implantation. To the best of the authors' knowledge, this is the first time this approach has been proposed for usage in cardiac applications.

Materials and Methods

All materials were either purchased from Sigma–Aldrich (Germany) or otherwise specified.

Scaffold Preparation

An electrospinning system (Fanavar Nano Meghyas Co. Ltd, Iran) was applied to generate the fiber scaffolds. Briefly, PCL and Gel were dissolved in acetic acid/formic acid (9:1) at a weight ratio of 1:1 to produce polymer solutions with a concentration of 18 wt.%. The formic acid/acetic acid solvent system yields fibers with significantly reduced diameter (10x smaller than chloroform) and

enables stable, reproducible electrospinning.⁴³ The solutions were then agitated at room temperature for 72 hours. The PCL-Gel solution was next mixed with different concentrations of β TCP nanoparticles (0.25, 0.5, 1, and 3 wt.%). Thereafter, the solution was filled into a 5 mL syringe to which an 18-gauge needle was attached. Using a syringe pump, the flow rate was adjusted to 0.1 ml/h with the applied voltage kept constant at 22 kV for each group. An aluminum foil was placed 10 cm from the needle tip as a collector. Each experiment was carried out at a relative humidity of 45% and room temperature. The vapor phase cross-linking process was performed by placing the electrospun scaffolds in a dryer containing 10 mL of 50% glutaraldehyde (GTA) solution at 25 °C for 12 h.⁴⁴ The scaffolds were subjected to a vacuum oven for one hour prior to the experiments to ensure complete evaporation of any remaining solvent. After cross-linking, the scaffolds were usually washed repeatedly for 24 h with phosphate buffered saline (PBS) to neutralize and remove unreacted GTA. Final drying was performed under vacuum at 45 °C to remove traces of moisture. The groups examined are listed in Table 1.

Scaffold characterizations

Physicochemical properties

The morphological properties of nanofiber scaffolds were tested using a scanning electron microscope (SEM; AIS2300C, South Korea). All groups were coated with a layer of gold before imaging. The fiber's diameter was assessed via the Image J software (National Institutes of Health, Bethesda, USA).⁴⁵ To examine the structural phases of the scaffolds, X-ray diffraction (XRD) was performed using a diffractometer (EQUINOX3000, Inel, France) with Cu- α radiation ($\lambda = 1.58897 \text{ \AA}$) at 40 kV and 40 mA. The scan rate was recorded at $0.08^\circ/\text{s}$ over the 2θ range of $5-100^\circ$.⁴⁶ The crystallite sizes were calculated using Debye-Scherrer's equation:

$$D = \frac{0.9\lambda}{\beta \cos \theta}$$

which λ represents the wavelength of Cu K α radiation and β denotes the full width at half maximum (FWHM) value.

Fourier transform infrared spectroscopy (FTIR) is a valuable analytical technique for identifying functional groups and analyzing details of covalent bonding. The

Table 1. Scaffold preparations and treated groups

Abbreviations	Scaffolds
PCL-Gel	18% PCL + 18% Gel
PCL-Gel- β TCP -0.25	18% PCL + 18% Gel + 0.25% β TCP
PCL-Gel- β TCP -0.5	18% PCL + 18% Gel + 0.5% β TCP
PCL-Gel- β TCP -1	18% PCL + 18% Gel + 1% β TCP
PCL-Gel- β TCP -3	18% PCL + 18% Gel + 3% β TCP

FTIR spectra of the samples were acquired using an FTIR spectrophotometer (PE1760x, Lumex, Canada) within the range of 4000–400 cm^{-1} with a scanning speed of 23 scans/min and a resolution of 1 cm^{-1} .⁴⁷ The tensile strength of the scaffolds was determined using a uniaxial tensile tester (Zwick/Roell, Germany) with a 10 N load cell and a strain rate of 1 mm/min.⁴⁸

Blood compatibility

Diluted and anticoagulated human blood was employed to explore the effect of the fibrous scaffolds on the blood. Specifically, 2 mL of freshly anti-coagulated human blood, 2.5 mL of normal saline (0.9%), and 0.2 mL of the anticoagulant blood diluted were added to the scaffolds and incubated at 37 °C for 60 min. Next, the mixture underwent centrifugation at a speed of 1500 rpm for a duration of 10 minutes. The resulting supernatants were measured for absorbance at 545 nm using a microplate reader (ELX808, BioTek, USA). To calculate the rate of hemolysis, we used an equation involving positive controls consisting of 0.2 mL of human blood diluted in 5 ml of deionized water (Dpc) and negative controls made up of 0.2 mL of human blood diluted in 5 ml of normal saline (Dnc). Dt represents the absorbance of the samples.⁴⁹

$$\text{Blood Hemolysis (\%)} = (D_t - D_{nc}) / (D_{pc} - D_{nc}) \times 100$$

Blood clotting index (BCI)

Fiber scaffolds were arranged in thin slices and placed at the bottom of a controlled 37 °C water bath in a beaker. Anticoagulated blood (100 μL) and a 0.2 M CaCl_2 solution (20 μL) were added to the scaffolds, followed by 25 mL of deionized water after 5 minutes. The obtained mixture was gently stirred at 37 °C with its absorbance measured at a wavelength of 545 nm. The experiment was repeated three times for each sample, with a control group containing no scaffolds. The level of blood clotting index was calculated using the following equation:

$$\text{Blood Clotting Index (\%)} = A_s / A_c \times 100$$

A_s represents the absorbance of the samples and A_c shows the absorbance of the control groups.⁵⁰

Biological assessments

Cardiomyocytes isolation

Cardiac cells were extracted from newborn rats aged 1 to 3 days, following a protocol approved by the Ethics Committee of Tarbiat Modares University, Iran (IR.MODARES.AEC.1404.003). Initially, the heart ventricles were collected and placed in ice-cold PBS. The tissues were chopped into pieces smaller than 1 mm^3 and then digested using a 0.1% (w/v) solution of collagenase type II (Worthington, NJ, USA) in Dulbecco's modified eagle medium (DMEM) for 10 minutes. The initial supernatant

was discarded, with this digestion procedure repeated until complete digestion was accomplished. The resulting mixture was filtered through a 100 μm cell strainer to separate cell clumps, after which the cells were centrifuged, resuspended in complete DMEM medium, and pre-plated in a T-75 flask coated with 0.1% gelatin for 2 hours. The non-adherent cells, primarily cardiac myocytes, were then collected and cultured in DMEM with high glucose, supplemented with 1% penicillin/streptomycin and 10% horse serum (Gibco).⁵¹

Cell viability analysis and morphology assessment

A cytocompatibility evaluation was conducted using the 3-(4,5-dimethylthiazol-2-yl)-2,5-diphenyl-2H-tetrazolium bromide (MTT) assay at 48, 72, and 120 hours. Briefly, each scaffold was sterilized under Ultraviolet (UV) light for 30 minutes on each side to ensure aseptic conditions were maintained. Next, 10^4 cells were combined in an expansion medium, transferred onto the scaffolds within 96-well culture plates, and incubated at 37°C with 5% CO_2 . At each time point, the scaffolds were rinsed with PBS, with a 150 μL solution of a 5:1 mixture of media and MTT (5 mg/mL in PBS) being added to each well, followed by incubation. After four hours, the medium was removed, and the formazan crystals were dissolved in dimethylsulfoxide (DMSO). The optical absorbance was assessed at a wavelength of 570 nm using a microplate reader (ELX808, BioTek, USA). At least three samples were averaged for each trial, with the cells on the tissue culture plate (TCP) serving as the control. Cell viability was expressed as a percentage compared to the control group.⁵² The morphology of CMs was inspected using SEM 48h after seeding. Samples were fixed in 2.5% glutaraldehyde in PBS for 1 hour, followed by a stepwise dehydration process using an ethanol series (30%, 50%, 70%, 90%, and 100%). Once the samples were sputter-coated with gold, SEM imaging was undertaken at different magnifications to assess fiber uniformity and cell morphology.⁵³

Quantitative real-time PCR

Five days after seeding, the gene expression profiles of cardiac cells on scaffolds were tested. The investigation focused on markers such as troponin T type 2 (TrpT2), the gap junction protein Connexin43 (Conx43), and actinin alpha 4 (Actn4) using quantitative real-time PCR (qRT-PCR). Total RNA was isolated from approximately 5 million cells lysed in 700 μL of RiboEX solution (GeneALL, cat. no. 302-001) designed for cardiac cells cultured on nanofibrous scaffolds. Thereafter, the isolated RNA was subjected to reverse transcription using the Easy cDNA Synthesis Kit (Parstous, Iran). Quantitative RT-PCR was performed using the SYBR Green QPCR Master Mix (YTA, Cat. No. YT2551) and Real-Time PCR System (Applied Biosystems, Lincoln, CA). The 20 μL reaction volume contained 10 μL SYBR Green Master Mix, 0.5 μL each of forward and reverse primers, 3 μL cDNA

template, and 6 μ L RNase-free water. Amplification was conducted at the annealing temperature. The changes in gene expression levels were carefully quantified compared to the control using the $2^{-\Delta\Delta CT}$ formula, employing Glyceraldehyde-3-phosphate dehydrogenase (GAPDH) as a housekeeping gene.⁵¹

Subcutaneous scaffold implantation

To assess the angiogenic potential *in vivo*, subcutaneous scaffold implantation was performed. Twelve male Naval Medical Research Institute (NMRI) mice, aged 7 to 8 weeks and weighing between 30 and 35 g, were utilized for this experiment. Three days prior to transplantation, cyclosporine (Novartis Pharma AG, Switzerland) was added to the animals' drinking water. A combination of xylazine (Alfasan, Netherlands; 0.02 mL/10 g body weight) and ketamine (Alfasan, Netherlands; 0.04 mL/100 g body weight) was administered intraperitoneally to induce general anesthesia. For transplantation, a small incision was made on the back of the mice with 15×15 mm² scaffolds implanted subcutaneously (Group 1: PCL-Gel; Group 2: PCL-Gel- β TCP-1), $n=3$ per group). The incision was then closed using a surgical suture. Following the procedure, the mice were recovered and had unrestricted access to food as well as water.⁵⁴ Finally, they were sacrificed after 2 and 4 weeks for the experiment.

Histological and immunohistochemical analysis

The implanted scaffolds were explanted along with the surrounding tissue, fixed in 10% buffered formalin for 48 hours, and subsequently transferred to PBS at 4 °C. Cellularization was evaluated by sectioning the fixed tissues into 5 μ m thick segments and staining them with hematoxylin and eosin (H&E). Images were obtained utilizing an AxioPlan microscope (Carl Zeiss GmbH, Germany) fitted with an AxioCam camera. The cell migration rate was evaluated as follows:

$$\text{Cell Migration Rate (\%)} = (W1 / W0) \times 100$$

which W1 represents the zone within the scaffold and W0 denotes the area of the entire scaffold.

The process of vascularization was visualized through immunohistochemical examination. Following deparaffinization and embedding in paraffin, the tissues were blocked with 3% (w/v) bovine serum albumin (BSA) in PBS at pH 7.4 for 20 minutes at 20 °C. The slides were incubated with the primary anti- Vascular Endothelial Growth Factor Receptor 2 (VEGFR2) antibody (1:100; Abcam) for 12 hours at 4 °C. The samples were then subjected to three rinses, each lasting five minutes, using PBS. A peroxidase-conjugated polymer staining kit containing antibodies to mouse and rabbit immunoglobulins was utilized to stain the samples. Positive cells were observed through applying the chromogen 3,3'-diaminobenzidine (DAB) (Vector Laboratories, Burlingame). The slides

were examined under a light microscope once the sections were dehydrated, mounted, and counterstained with Hematoxylin.⁵⁵ At least four scaffold sections and six images per section were assessed to collect data.

Statistical analysis

Statistical analyses were conducted using two-way ANOVA, with post-hoc comparisons performed by Tukey's test to assess within-group differences over time. Calculations were carried out using GraphPad Prism software (version 8.1.2). The results are expressed as mean \pm standard deviation (SD). A P-value of less than 0.05 was considered to indicate statistical significance. A minimum of three samples were examined for each experiment.

Results and Discussion

The loss of cardiomyocytes, a hallmark of heart disease, results in significant cardiac dysfunction, ultimately culminating in heart failure. Despite major advances in treatment, the prognosis for heart failure remains bleak, as conventional therapies do not address the abnormalities in the number of heart muscle cells.⁵⁶ Multiple studies have indicated that cardiomyocyte proliferation is essential for natural heart regeneration. To enhance cardiac function following injury or to prevent further deterioration, substantial efforts have been made to support the proliferation of mammalian cardiomyocytes.^{57,58} The goal of cardiac tissue engineering is to replace or repair damaged heart muscle cells effectively. Thus, the use of scaffolds in various shapes, such as patches, may provide a suitable environment for cardiomyocytes.^{59,60} PCL is a synthetic biodegradable polymer with a long degradation time of 2 to 4 years, which may not be in accordance with the desired time for cardiac tissue repair, typically several months to a year. This problem has been a focus in tissue engineering research, where PCL is more desirable because of its better mechanical stability but will often need the incorporation of other materials, such as Gel or HA, to facilitate its degradation. In cardiac tissue engineering, this incompatibility can cause the scaffold to persist at the injury site and provoke an inflammatory response.⁶¹ The incorporation of Gel with PCL enhances cellular adhesion and diminishes the degradation rate in comparison to unmodified PCL. Furthermore, the introduction of minerals like HA or β TCP into the polymer scaffolds modulates the degradation rate by elevating solubility in aqueous environments.⁶² This study presents compelling evidence that the incorporation of β TCP into PCL-Gel scaffolds significantly boosts their ability to support cardiomyocyte growth and function. Electrospun nanofiber patches can be used to transport cardiac progenitor cells or functional cardiomyocytes. In 2021, Sridharan and colleagues created and researched fibrous scaffolds with a coaxial PCL/gel structure using

the electrospinning technique. The results revealed that human induced pluripotent stem cells (iPSCs) can be cultured on these scaffolds and developed into functional cardiomyocytes.⁶³

Physicochemical properties

SEM images were utilized to explore the influence of β TCP on the microscopic structure of PCL-Gel fibers. The images presented the nanofibers of PCL-Gel, PCL-Gel- β TCP-0.25, PCL-Gel- β TCP-0.5, PCL-Gel- β TCP-1, and PCL-Gel- β TCP-3 with mean diameters of 45.01 ± 2.82 , 53.66 ± 7.45 , 81.12 ± 9.75 , 99.96 ± 15.34 , and 100.91 ± 11.69 μm , respectively (Fig. 1). A smaller diameter results in a larger surface area in fibrous scaffolds, making larger space for cell attachment, simulating ECM growth for various cells *in vivo*.⁶⁴ Pores facilitate drug transport and tissue angiogenesis, enabling cell infiltration, oxygen transport, and nutrient spread throughout the tissue.⁶⁵

XRD analysis was applied to examine the structural crystalline phase of the fabricated scaffolds (Fig. 2). In general, PCL is a semicrystalline homopolymer with diffraction peaks at $2\theta = 21.9^\circ$ and 24.2° , corresponding to the (110) and (200) planes of the orthorhombic crystal structure.^{66,67} The weakly intense peaks in the XRD pattern of the sample without β TCP are owing to the low crystallinity of the PCL-Gel structure. By incorporating the β TCP into the composite, crystalline peaks appeared at 21.6° , 23.9° , 29.7° , 46.7° , and 49.3° , corresponding to (0240), (1010), (3000), (4010), and (4160) planes for the β TCP phase in the rhombohedral structure.^{68,69} It can also be observed that the intensity of the crystalline peaks grows with increasing β TCP content in the chemical composition of the composite. The crystallite sizes of β TCP in the samples with concentrations of 0.25, 0.5, 1, and 3 wt% were measured at 16.2, 16.5, 17.2, and 17.7 nm, respectively. This suggests that a higher concentration of the bio-ceramic contributes to a growth in the crystallite size of the composite phase.

FTIR spectra of the scaffolds are illustrated in Fig. 3A. The absorption peaks observed at 3290 cm^{-1} and 3080 cm^{-1} are associated with the stretching vibration of O-H and N-H bonds present in the Gel. Meanwhile, the peaks at 2940 cm^{-1} and 2870 cm^{-1} correspond to the asymmetric and symmetric stretching vibration of aliphatic C-H bonds found in both Gel and PCL structures.^{70,71} The characteristic peak at 1730 cm^{-1} is ascribed to the stretching vibration of C=O in PCL,⁷² while the localized peak at 1640 cm^{-1} can be attributed to the stretching vibration of the C=C bond in aromatic rings of Gel and/or bending vibration of the O-H bond in retained moisture.⁷³ The peaks appearing at 1540 cm^{-1} , 1450 cm^{-1} , and 1370 cm^{-1} are assigned to the bending vibration of N-H and C-H bonds, respectively, and the absorption peak at about 1299 cm^{-1} is because of the stretching vibration of C-N in Gel.^{74,75} In addition, the absorption peaks at 1240 cm^{-1}

and 1170 cm^{-1} are associated with the stretching vibration of C-OH and C-O-C bonds in Gel and are attributed to the peaks within the wavenumber range from 800 cm^{-1} to 1100 cm^{-1} the stretching vibration functional carbon-oxygen groups as well as phosphorus-oxygen bonds in the β TCP structure. The spectra demonstrate that the intensity of the localized peaks in the wavenumber range increased with elevating the β TCP concentration in the nanocomposite due to the presence of more P=O bonds in their chemical composition. It can also be seen that the bending vibration of the P=O bond causes a new peak at around 730 cm^{-1} , being further evidence for the presence of the phosphate-based structure in the β TCP-containing samples.⁷⁶ The observable peak at around 630 cm^{-1} is linked to the bending vibration of C-H bonds in aromatic structures.⁷⁵ The higher intensity of the peak for the PCL-Gel samples can be attributed to the interaction of the β TCP structure with the aromatic rings, resulting in a decline in the peak intensity in the presence of the bio-ceramic structure.

Mechanical properties

The mechanical characteristics and stress-strain graphs of fiber scaffolds are presented in Fig. 3B and Table 2. The point at which the scaffold fails is indicated by the maximum tensile stress. The PCL-Gel, PCL-Gel- β TCP-0.25, PCL-Gel- β TCP-0.5, PCL-Gel- β TCP-1, and PCL-Gel- β TCP-3 fiber scaffolds showed tensile strength values of 1.35 ± 0.03 MPa, 1.74 ± 0.07 MPa, 2.40 ± 0.11 MPa, 1.65 ± 0.09 MPa, and 1.50 ± 0.06 MPa, respectively. Such a behavior is usually related to particle agglomeration and decreased continuity of the polymer at higher levels of ceramics, which create sites of stress concentration and enhance brittleness. For example, in bone tissue engineering scaffolds, high β TCP concentration disordered the PCL/PLGA matrix and resulted in decreased mechanical stability at the expense of initial enhanced strength at low TCP concentrations. Likewise, Poly (3-hydroxybutyrate) PHB/PCL-TCP blends also exhibited reduced ductility and enhanced brittleness at elevated TCP concentrations due to inadequate interfacial bonding between the polymer and ceramic phases.^{77,78} Adjusting the ratio of PCL to Gel can increase flexibility without sacrificing tensile strength. Cardiac patch studies have ascertained that a 50:50 PCL and Gel composite increases elasticity and cell compatibility without sacrificing structural integrity. Specifically, the hydrophilic properties of gelatin act against the hydrophobic properties of PCL, facilitating homogeneous distribution of β TCP and preventing clumping at higher concentrations.⁷⁹ The incorporation of β TCP altered the final tensile strength of the scaffolds depending on the concentration, indicating a rise in their breaking strength up to a concentration of 0.5%. Further, upon adding this ceramic to the manufactured composite and elevating its concentration based on the

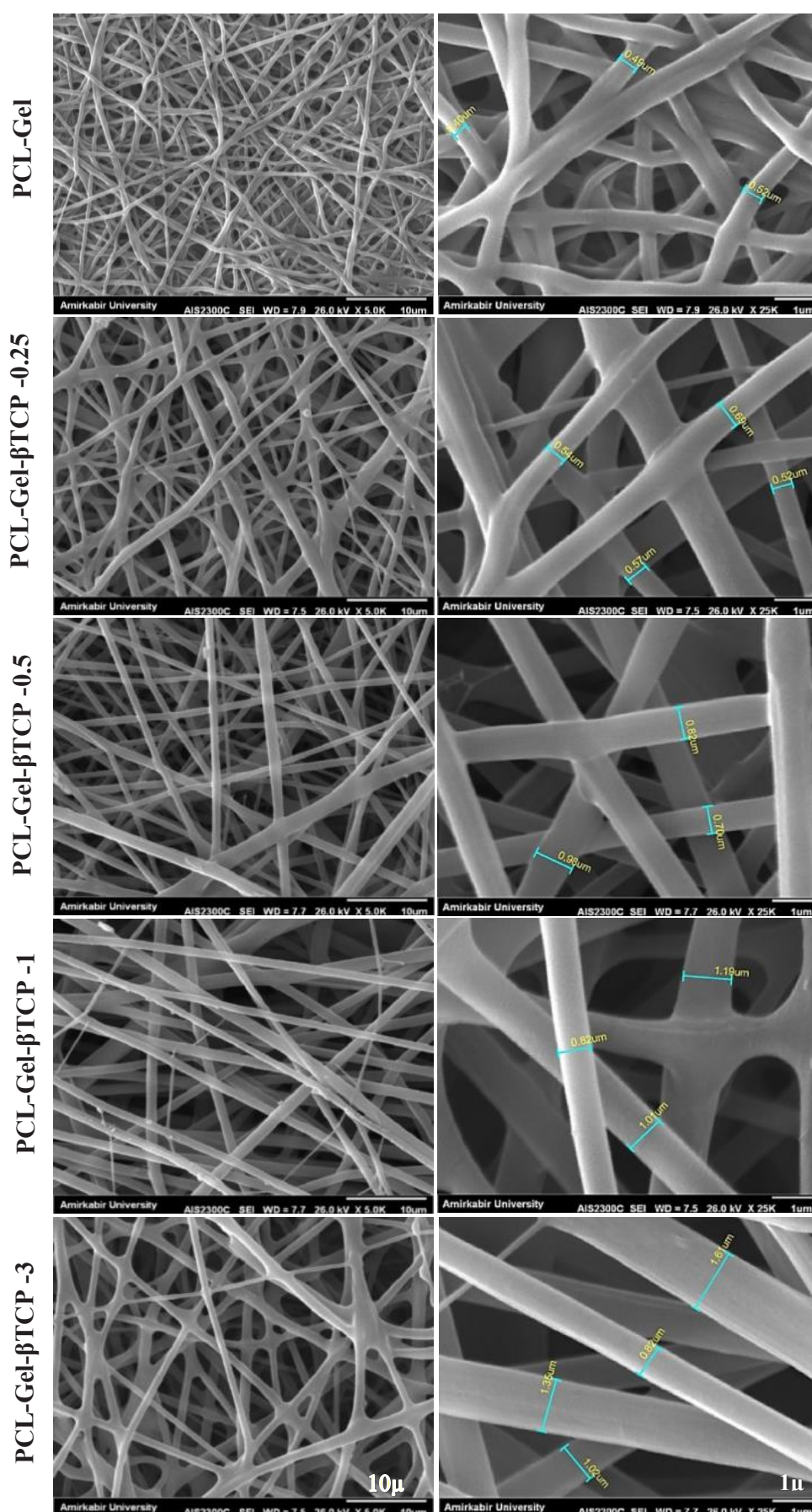


Fig. 1. SEM images of prepared scaffolds with different concentrations of β TCP (from left to right 5 and 25 kX magnifications).

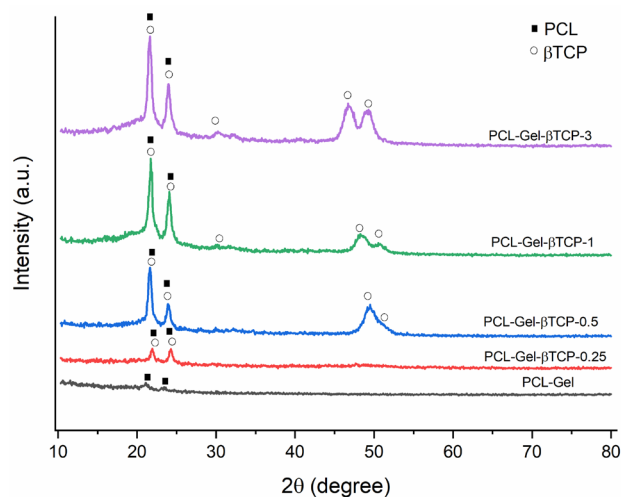


Fig. 2. X-ray diffraction (XRD) analysis of the fabricated scaffold groups.

elastic modulus diagram, it is possible to achieve higher fragility and brittleness of the composition. Meanwhile, the obtained elastic modulus was within the range of a tissue-engineered cardiac patch.⁸⁰

Blood compatibility and blood clotting index (BCI)

To assess the blood compatibility of cardiac patches, the hemolysis effect is a key aspect that should be evaluated. The PCL-Gel, PCL-Gel-βTCP-0.25, PCL-Gel-βTCP-0.5, PCL-Gel-βTCP-1, and PCL-Gel-βTCP-3 fiber scaffolds presented a hemolysis percentage of 3.88 ± 0.19 , 3.67 ± 0.12 , 3.84 ± 0.15 , 3.96 ± 0.08 , and 3.44 ± 0.13 , respectively (Fig. 4A). There is no statistically significant difference between the treatment groups, and the percentage of hemolysis is lower than 5% in all samples tested.

To assess the antithrombogenic properties of a material concerning human blood, the BCI was employed in research. Typically, the BCI value correlates inversely with the coagulation effect of the material, with lower values indicating improved anti-thrombogenic properties.⁸¹ To evaluate clot formation, human blood drops were applied to fibers and after 60 minutes, absorbance was measured to determine the amount of free hemoglobin released from clotted blood (Fig. 4B). Absorbance values were converted to percent free hemoglobin and calculated as BCI values for each sample. The PCL-Gel, PCL-Gel-βTCP-0.25, PCL-Gel-βTCP-0.5, PCL-Gel-βTCP-1, and PCL-Gel-βTCP-3 fiber scaffolds presented a blood clotting index of 70.05 ± 3.12 , 61.17 ± 2.52 , 60.09 ± 1.85 , 59.71 ± 1.99 , and 45.29 ± 5.33 , respectively (Fig. 4C). According to these results, as the amount of βTCP in the composites increased, the amount of BCI decreased.

Zamani et al reported that the rate of hemolysis is affected by the compatibility of different materials; the level of hemoglobin in plasma is represented by the extent of damage caused by erythrocytes. Based on previous studies, the critical hemolysis limit is less than 5%.⁸² In this study, the hemolysis rate of PCL gel scaffolds with different

Table 2. Mechanical properties of PCL-Gel containing various concentrations of βTCP

Groups	Ultimate tensile stress (MPa)
PCL-Gel	1.35 ± 0.03
PCL-Gel-βTCP -0.25	1.74 ± 0.07
PCL-Gel-βTCP -0.5	2.40 ± 0.11
PCL-Gel-βTCP -1	1.65 ± 0.09
PCL-Gel-βTCP -3	1.50 ± 0.06

concentrations of βTCP was lower than 5%, showing the blood compatibility of the developed composite materials. In cardiac tissue engineering, the non-clotting or non-thrombogenic ability of materials is crucial to prevent formation of blood clots on engineered tissues. Otherwise, implanted devices can obstruct blood vessels, which can lead to dangerous conditions such as thrombosis and stroke. In order for heart tissue scaffolds and artificial constructs to function effectively, they need to integrate seamlessly into the native tissue. The formation of blood clots can generate barriers, inflammatory reactions, or fibrosis that prevent proper integration.⁸³ The BCI test was employed to test the coagulation activity of materials. The lower the BCI value, the more effective the coagulation effect of the scaffolds.⁸⁴ Based on previous research, βTCP exhibits certain coagulation characteristics. It interacts with blood components such as platelets, potentially resulting in localized clotting effects. When it comes into contact with blood, its calcium content and surface characteristics can promote platelet adhesion and activation, which may support the formation of clots.⁸⁵ Thus, based on the results of this study, βTCP at various concentrations had a negative effect on the coagulation process, so as the amount of βTCP increased, the amount of BCI diminished, complicating its usage at a dose of 3%. For this reason, we used the composite with 1% βTCP for *in vivo* testing, which resulted in no significant difference from other previous treatment groups in coagulation induction.

MTT assay

Isolated cardiac cells were employed to test the prepared scaffolds for possible cytotoxic effects.⁸⁶ The MTT assay was used to evaluate using the cytocompatibility of CMs cultured on PCL-Gel and βTCP-containing scaffolds at different concentrations. As displayed in Fig. 5, the findings indicated that all samples containing βTCP in their composition exhibited significantly enhanced viability at the 24, 72, and 120-hour intervals when compared to the group lacking βTCP (PCL-Gel). Further, an increase in the concentration of βTCP within the composite scaffolds was associated with greater viability. Hence, enhancing cell viability indicated that there was no toxicity associated with the combination of the prepared scaffolds, as this value consistently exceeded 98% for all samples at 120 hours following seeding.

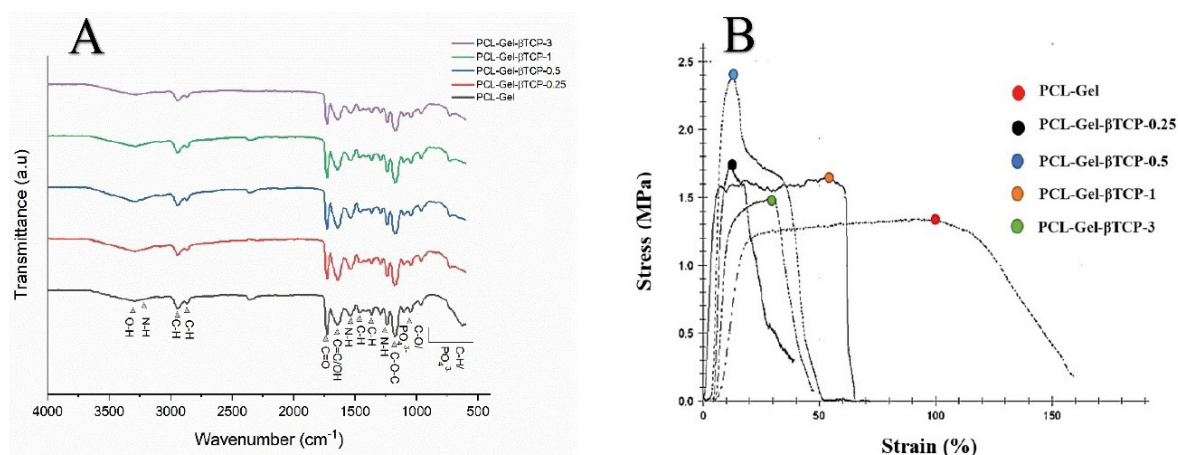


Fig. 3. (A) FTIR absorbance spectra of the fabricated scaffolds in 400 to 4400 cm⁻¹. **(B)** Mechanical tensile Stress-Strain curve of prepared scaffolds.

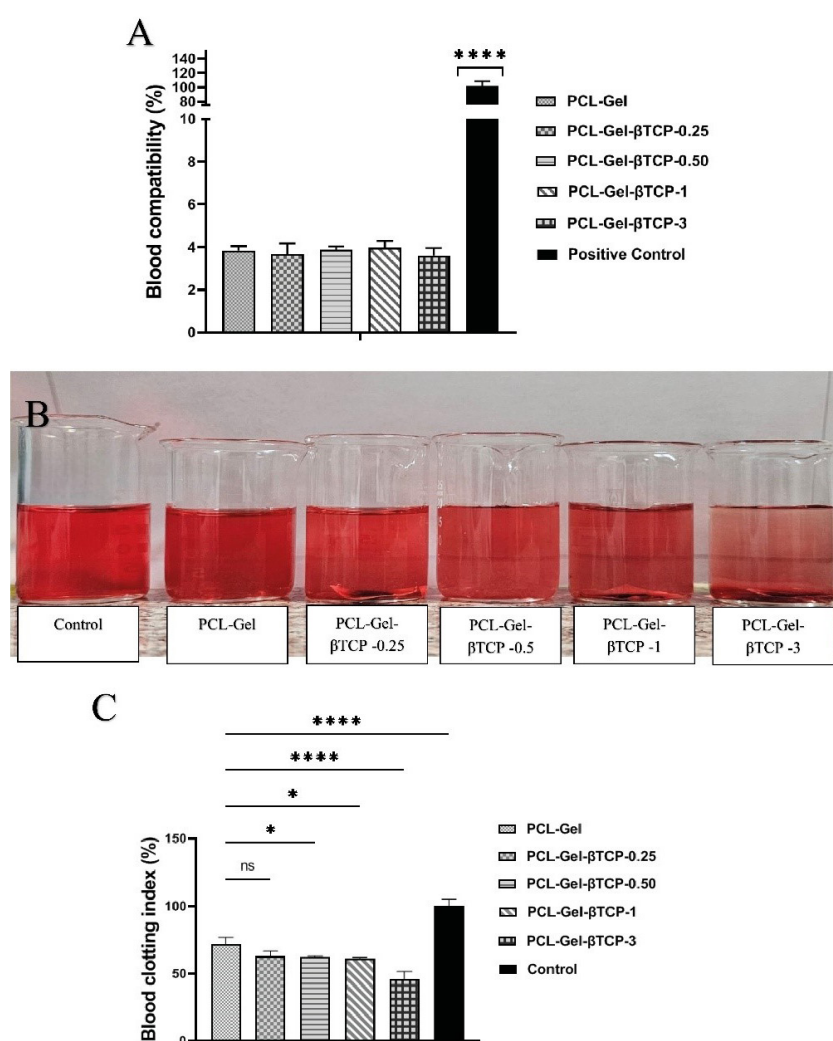


Fig. 4. (A) The percentage of blood compatibility of the fabricated scaffolds in comparison to the positive control. **(B)** Macroscopic visualization of blood-treated group, **(C)** Blood Clotting Index of the prepared scaffolds. * $P < 0.05$, and **** $P < 0.0001$.

Scanning electron microscopy

SEM images of cardiomyocytes were captured 48 hours post-seeding. As depicted in Fig. 6, the micrographs indicated that each sample promoted cell attachment. Notably, an increase in the concentration of βTCP within

the prepared scaffolds caused the cells to exhibit a flatter morphology. The improved cell attachment observed for scaffolds with higher βTCP concentrations suggests that βTCP enhances the polymeric structure of the scaffold in a dose-dependent manner.⁸⁷

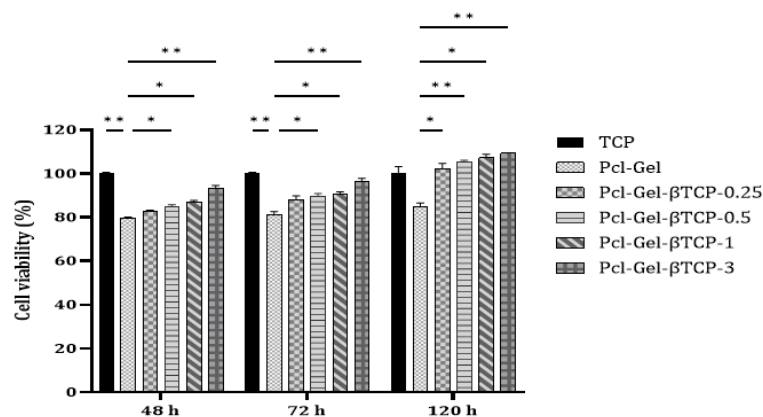


Fig. 5. MTT assay results of cardiomyocyte seeded on prepared samples after 48, 72, and 120 hours. * $P < 0.05$ and ** $P < 0.01$.

Gene Expressions Analysis

The expression profile of the cardiac gene markers for cardiomyocytes seeded on the scaffolds was inspected using qRT-PCR and presented in Fig. 7. The oligonucleotide primer pairs used are listed in Table 3. As can be observed, the corresponding gene expression was statistically increased in all scaffolds compared with the control. This value was more significant for PCL-Gel-βTCP-3, particularly for the TrpT2 gene marker ($P < 0.001$).

The results showed a significant increase in cell viability at higher βTCP concentrations, especially at 3%, suggesting that βTCP significantly improves the performance of the scaffold in supporting cell proliferation. This trend was consistently observed across different time points and shows a sustained positive effect of βTCP on cell growth, consistent with previous studies.^{88,89} This conclusion is further supported by gene expression analysis, which shows a significant increase in markers critical for cardiomyocyte function at different βTCP levels. These results suggest that βTCP not only increases cell viability but also promotes specific cellular functions essential for cardiac tissue engineering.⁹⁰ Actinin-4 (Actn4) is essential for cardiac repair and cardiomyocyte functions, contributing to structural support, regulation of cell motility, ECM remodeling, and promoting cardiomyocyte proliferation. These roles are crucial for the effective regeneration and function of cardiac tissue.⁹¹ Connexin 43 (Conx43) is a critical gap junction protein that plays a central role in cardiac repair by regulating intercellular communication, electrical conduction, and cellular signaling in the heart.⁹² Furthermore, Conx43 is involved in promoting cardiomyocyte proliferation, regeneration, and survival in experimental models.⁹³ Troponin T type 2 (TrpT2) plays a role in calcium hemostasis and signaling within cells, which is critical for function and repair. Improvements in gene expression markers important for cardiomyocyte function suggest that βTCP-enriched scaffolds hold promise for cardiac tissue engineering.⁹⁴ βTCP in composites (PCL-Gel) resulted in an increase

in the expression level of these genes with increasing concentration, which may be useful for cardiac tissue engineering patches.

Histological analysis

Based on the results obtained from physicochemical and biological investigations, the PCL-Gel-βTCP -1 sample was selected for in vivo evaluations, and its results were compared with those of the sample without βTCP. Twelve NMRI mice were used for the experiment and were sacrificed after 2 and 4 weeks. The H&E images demonstrated improved perivascular localization, as shown in Fig. 8A, with both scaffolds exhibiting cellularization after four weeks.

Chen and colleagues reported the use of electrospun PCL/Gel nanofiber scaffolds loaded with graphene. The results of CCK-8 assays and histopathological staining indicated that cells on the hybrid scaffolds exhibited optimal culture and survival when the mass fraction of graphene was below 0.5%. Following implantation in rats for 4, 8, or 12 weeks, H&E staining demonstrated the absence of inflammatory cell accumulation around the nanomaterials.⁹⁰ The newly formed blood vessels in the cellularized area were examined using immunofluorescence staining with VEGFR2 (Fig. 8B). Furthermore, the PCL-Gel-βTCP-1 scaffold showed a significantly higher cell migration rate throughout the evaluation period (Fig. 8C) compared to the PCL-Gel sample, reaching approximately 68% after 4 weeks. The PCL-Gel-βTCP-1 scaffold therefore exhibited a significantly increased cell migration rate ($P < 0.01$). As adequate cellularization is essential for efficient vascularization,⁹⁵ the PCL-Gel-βTCP-1 scaffold used in this research created favorable conditions for cell infiltration and migration due to its appropriate composition. Additionally, an increase in capillary formation was observed on this scaffold, which supports the findings of cell viability highlighted in the MTT assay. It appears that this scaffold provides a suitable microenvironment for cell homing and proliferation.

Vascularization plays a crucial role in cardiac repair and

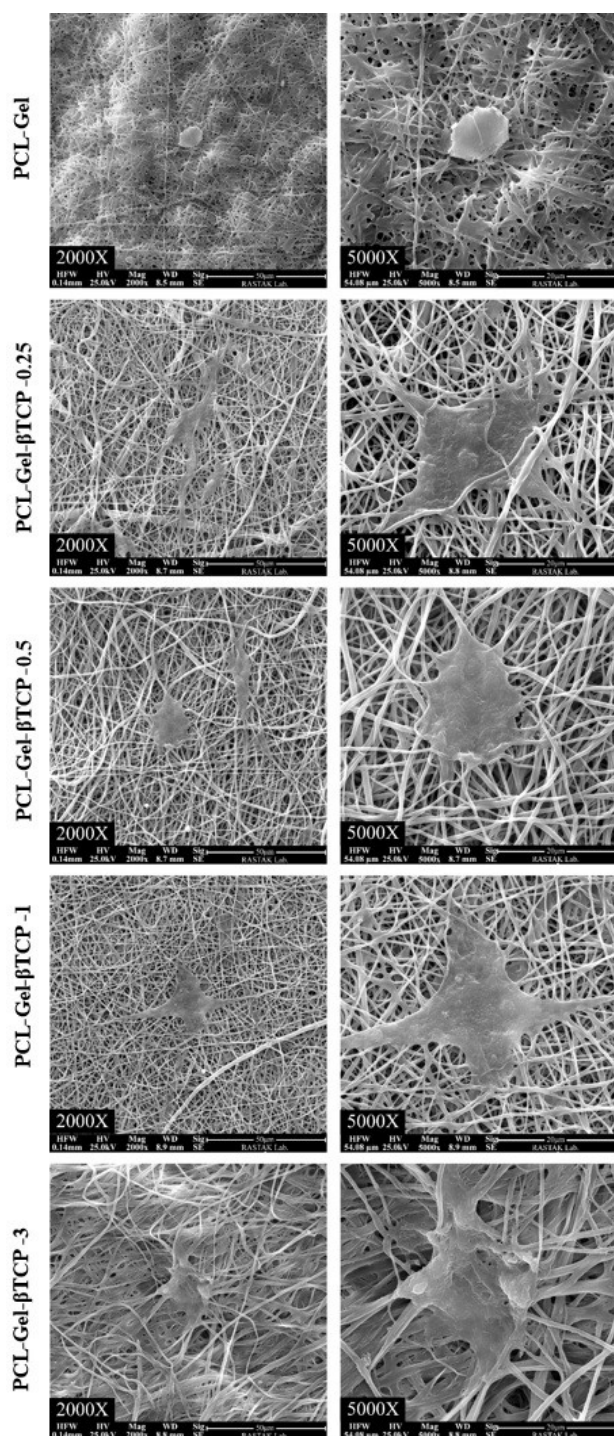


Fig. 6. Morphology of cardiac cells cultured on scaffolds following 48 hours post-seeding with different magnifications.

regeneration. β TCP has been shown to have beneficial effects on angiogenesis by acting through the PI3K/Akt pathway.⁹⁶ This pathway improves the functionality, movement, adherence, and proliferation of endothelial cells. Consequently, this could be advantageous for promoting vascularization and the integration of the cardiac patch into the host tissue.^{87,97} Our results from post-implantation tests indicated that the PCL-Gel- β TCP-1 scaffold increased cellularization and

demonstrated improved cell migration compared to PCL-Gel.⁹⁸ This suggests that the incorporation of β TCP into the PCL-Gel scaffold enhances the bioactive properties of the composite, promoting accelerated cell infiltration and cellularization.⁹⁹ Furthermore, in the current study, the PCL-Gel- β TCP-1 scaffold exhibited enhanced angiogenic potential, as evidenced by the increased expression of VEGF and the formation of capillary-like structures.¹⁰⁰ This effect is attributed to the presence of β TCP, which stimulates the production of angiogenic factors and promotes endothelial cell migration.¹⁰¹ Additionally, the porous structure of the scaffolds acts as a reservoir for retaining the essential Ca^{2+} ions needed to attract mesenchymal stem cells (MSCs), myoblasts, myoendothelial cells, and pericytes for neovascularization process.¹⁰²

The hydrophobic nature of PCL limits its cell affinity, which can be improved through surface modifications such as NaOH treatment, shown to enhance endothelial cell adhesion like human umbilical vein endothelial cell (HUVECs) and PCL biocompatibility.¹⁰³ β TCP scaffolds also demonstrate pro-angiogenic properties, promoting HUVEC infiltration, migration, proliferation, and upregulating angiogenic markers like CD31, especially in channel-like architectures, indicating strong neovascularization potential.¹⁰⁴ In cardiac tissue engineering, incorporating cell types such as cardiac fibroblasts—key for ECM deposition but potentially contributing to pathological remodeling if dysregulated—and hiPSC-derived cardiomyocytes (hiPSC-CMs)—which mimic patient-specific genetics and enable drug testing—can improve regenerative outcomes.^{105,106} Gelatin-based hydrogels support hiPSC-CM culture; matrices with suitable stiffness and degradation rates enhance network formation, expression of contractile proteins, and contraction velocity, emphasizing the importance of mechanical properties for functional cardiac tissues.¹⁰⁷

Based on these insights, future research will focus on developing a multicellular co-culture system incorporating endothelial cells, cardiac fibroblasts, and hiPSCs within our tissue-engineered constructs. This strategy aims to better mimic the native cellular complexity of the myocardium, promote more physiologically relevant cell-cell interactions, and ultimately improve the translational relevance of engineered cardiac tissues.

While β TCP has been extensively used in bone repair due to its osteoconductivity¹⁰⁸, biodegradability,¹⁰⁹ and biocompatibility,^{110,111} it is also a promising candidate for cardiac tissue engineering. Its controlled dissolution facilitates gradual material replacement by native tissue, while the release of bioactive Ca^{2+} plays a critical role in modulating the local microenvironment. Ca^{2+} ions released during β TCP degradation enhance angiogenesis and myocardial repair by activating signaling pathways in endothelial and cardiac cells.^{40,112} In addition, Ca^{2+} acts as

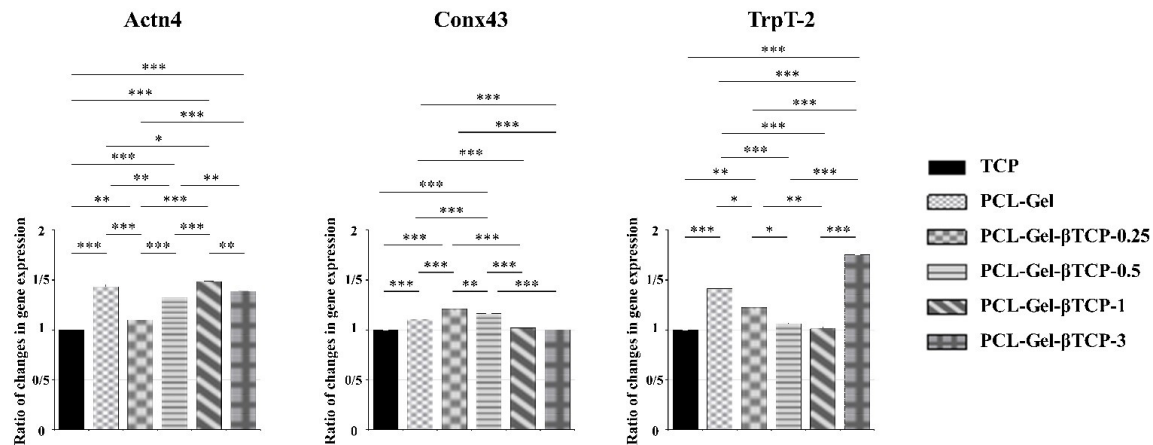


Fig. 7. Gene Expression Analysis. The bar graphs compare gene expression in cardiomyocytes on TCP control and PCL-Gel scaffolds with varying β TCP concentrations (* $P < 0.05$, ** $P < 0.01$, *** $P < 0.001$).

Table 3. Primers used for qRT-PCR

Genes	Abbreviations	Primer Sequence (5'-3')	Annealing (°C)
Troponin T type 2	TrpT ₂	F: CGACCACCTGAATGAAGACC R: TTTCTGCTGCTGAACCTTTCC	59.4
Connexin43	Conx ₄₃	F: TATGTGATGAGGAAGGAAGAGAAG R: TTGAAGATGCTGATGCTGATGATGTAG	59.3
Actinin Alpha 4	Actn ₄	F: CGGGATGGGCTCAAACCTATG R: GATGTCTTGGATGGCGAACC	59.8
Glyceraldehyde-3-phosphate dehydrogenase	GAPDH	F: CTCATTTCTGGTATGACA R: CTTCTCCCGTGCTCTTGCT	59.5

the key link between electrical excitation and contraction in cardiomyocytes while regulating gene transcription and other critical cellular functions.⁴⁰ Experimental studies support the angiogenic potential of β TCP. In vitro, β TCP scaffolds have been shown to promote HUVEC infiltration, proliferation, and migration. Additionally, the expression of angiogenic marker CD31 and migration-associated protein α 5 is upregulated on β TCP scaffolds with channel-like architectures, indicating a strong capacity to stimulate neovascularization.¹⁰⁴ In vivo, unidirectional porous β TCP (UDPTCP) has demonstrated significant vascularization potential. Three weeks post-implantation, UDPTCP structures were fully infiltrated by capillaries, with endothelial cells, pericytes, and basement membranes contributing to the formation of a mature vascular network.¹¹³ Despite these biological advantages, the inherent brittleness and stiffness of β TCP limit its utility as a standalone material in soft tissue applications like cardiac repair. To overcome these mechanical limitations, β TCP is often integrated into composite scaffolds with pliable, biodegradable polymers such as PCL or Gel. These composites provide improved flexibility, prevent structural failure, enable tunable degradation kinetics, and enhance cellular compatibility. Supporting this composite strategy, chitosan/calcium silicate-based cardiac patches have demonstrated therapeutic efficacy in post-infarction models by promoting cardiomyocyte activation and enhancing myocardial function through the synergistic

effects of bioactive ion release and aligned nanostructural features. In vivo findings further confirm reduced scar tissue formation and increased angiogenesis, reinforcing the therapeutic potential of ion-releasing, nanostructured biomaterials for cardiac tissue engineering.¹¹⁴ Thus, polymer/ceramic composite patches incorporating β TCP represent a promising platform for myocardial repair. Integrating controlled biodegradability, ion-mediated bioactivity, and customizable mechanical properties, β TCP-reinforced composites may support structural regeneration and functional restoration of infarcted myocardium.

Further research is needed to optimize composite formulations. Key areas include fine-tuning its degradation rate, enhancing angiogenic signaling, and exploring combination therapies with growth factors to maximize regenerative outcomes. *In vivo* assessments utilizing an animal model of heart attack are also essential to confirm the effectiveness of the created patches in regeneration process, as well.

Conclusion

Overall, the incorporation of β TCP into PCL-Gel scaffolds notably enhanced their cytocompatibility and functional support for cardiomyocytes, underscoring its potential as a promising material for cardiac tissue engineering. The scaffold with 1% β TCP demonstrated superior cell proliferation, vascularization, and

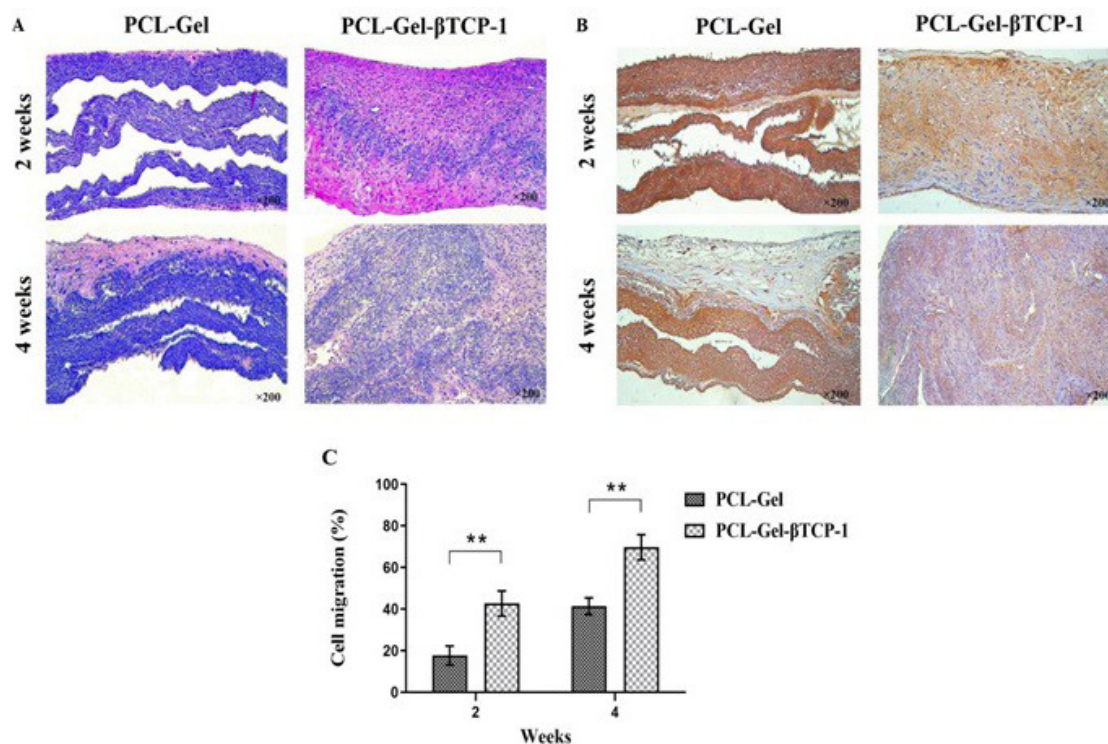


Fig. 8. (A) H & E staining of the scaffolds, **(B)** Immunohistochemistry staining of the scaffolds for VEGFR2, and **(C)** quantitative analysis of cell migration after 2- and 4-week subcutaneous implantation. (** $P < 0.01$).

migration, highlighting its capacity to promote tissue regeneration effectively. These findings corroborate previous studies that have shown β TCP's beneficial role in scaffold performance, particularly in facilitating cell attachment and angiogenesis. Looking forward, future research should aim to optimize β TCP concentrations and explore synergistic effects with other biocompatible materials to further refine scaffold properties. Long-term *in vivo* studies are essential to evaluate the durability, the potential risk of calcification, integration, and functional outcomes of such scaffolds in cardiac repair. Additionally, investigating scalable fabrication methods and assessing the clinical safety and efficacy of these composites will be critical steps toward translating this promising approach into viable therapeutic strategies for patients suffering from ischemic heart diseases.

Authors' Contribution

Conceptualization: Mahnaz Fathi, Nafiseh Baheiraei.

Data curation: Mahnaz Fathi, Sepehr Zamani, Hossein Eyni, Mehdi Razavi.

Formal analysis: Majid Salehi, Sepehr Zamani, Hossein Eyni.

Funding acquisition: Nafiseh Baheiraei.

Investigation: Mahnaz Fathi, Majid Salehi.

Methodology: Mahnaz Fathi.

Project administration: Nafiseh Baheiraei.

Resources: Nafiseh Baheiraei.

Supervision: Nafiseh Baheiraei.

Validation: Nafiseh Baheiraei, Nahid Moradi.

Writing—original draft: Nahid Moradi.

Writing—review & editing: Nafiseh Baheiraei, Nahid Moradi, Mehdi Razavi

Research Highlights

This study demonstrates that incorporating 1% β -tricalcium phosphate into PCL-Gel fibers creates an optimal cardiac patch scaffold, promoting cell proliferation, angiogenesis, and vascularization, with excellent biocompatibility and potential for advancing cardiac tissue engineering.

Competing Interests

The authors declare no conflict of interest.

Ethical Approval

This research was performed according to a protocol approved by the Ethics Committee of Tarbiat Modares University, Iran (IR.MODARES.REC.1399.188).

Funding

This work has been supported by the Center for International Scientific Studies and Collaboration (CISSC), Ministry of Science Research and Technology of Iran (grant number: 4020647).

References

1. Tsao CW, Aday AW, Almarzooq ZI, Alonso A, Beaton AZ, Bittencourt MS, et al. Heart disease and stroke statistics-2022 update: a report from the American Heart Association. *Circulation* 2022; 145: e153-e639. doi: 10.1161/cir.0000000000001052.
2. Schirone L, Forte M, Palmerio S, Yee D, Nocella C, Angelini F, et al. A review of the molecular mechanisms underlying the development and progression of cardiac remodeling. *Oxid Med Cell Longev* 2017; 2017: 3920195. doi: 10.1155/2017/3920195.
3. Jawad H, Ali NN, Lyon AR, Chen QZ, Harding SE, Boccaccini AR. Myocardial tissue engineering: a review. *J Tissue Eng Regen Med* 2007; 1: 327-42. doi: 10.1002/term.46.
4. Hubbell JA. Biomaterials in tissue engineering. *Biotechnology (N Y)* 1995; 13: 565-76. doi: 10.1038/nbt0695-565.

5. Edrisi F, Baheiraei N, Razavi M, Roshanbinfar K, Imani R, Jalilnejad N. Potential of graphene-based nanomaterials for cardiac tissue engineering. *J Mater Chem B* **2023**; 11: 7280-99. doi: 10.1039/d3tb00654a.
6. Adapala RK, Kanugula AK, Paruchuri S, Chilian WM, Thodeti CK. TRPV4 deletion protects heart from myocardial infarction-induced adverse remodeling via modulation of cardiac fibroblast differentiation. *Basic Res Cardiol* **2020**; 115: 14. doi: 10.1007/s00395-020-0775-5.
7. Chang T, Liu C, Lu K, Wu Y, Xu M, Yu Q, et al. Biomaterials based cardiac patches for the treatment of myocardial infarction. *J Mater Sci Technol* **2021**; 94: 77-89. doi: 10.1016/j.jmst.2021.03.062.
8. Wu T, Liu W. Functional hydrogels for the treatment of myocardial infarction. *NPG Asia Mater* **2022**; 14: 9. doi: 10.1038/s41427-021-00330-y.
9. Baheiraei N, Razavi M, Ghahremanzadeh R. Reduced graphene oxide coated alginate scaffolds: potential for cardiac patch application. *Biomater Res* **2023**; 27: 109. doi: 10.1186/s40824-023-00449-9.
10. Shojaie S, Rostamian M, Samadi A, Sabbagh Alvani MA, Khonakdar HA, Goodarzi V, et al. Electrospun electroactive nanofibers of gelatin-oligoaniline/poly(vinyl alcohol) templates for architecting of cardiac tissue with on-demand drug release. *Polym Adv Technol* **2019**; 30: 1473-83. doi: 10.1002/pat.4579.
11. Locarno S, Eleta-Lopez A, Lupo MG, Gelmi ML, Clerici F, Bittner AM. Electrospinning of pyrazole-isothiazole derivatives: nanofibers from small molecules. *RSC Adv* **2019**; 9: 20565-72. doi: 10.1039/c9ra02486g.
12. Chow LW. Electrospinning functionalized polymers for use as tissue engineering scaffolds. *Methods Mol Biol* **2018**; 1758: 27-39. doi: 10.1007/978-1-4939-7741-3_3.
13. Mehrabi A, Baheiraei N, Adabi M, Amirkhani Z. Development of a novel electroactive cardiac patch based on carbon nanofibers and gelatin encouraging vascularization. *Appl Biochem Biotechnol* **2020**; 190: 931-48. doi: 10.1007/s12010-019-03135-6.
14. Schmitt PR, Dwyer KD, Coulombe KKK. Current applications of polycaprolactone as a scaffold material for heart regeneration. *ACS Appl Bio Mater* **2022**; 5: 2461-80. doi: 10.1021/acsabm.2c00174.
15. Shin M, Ishii O, Sueda T, Vacanti JP. Contractile cardiac grafts using a novel nanofibrous mesh. *Biomaterials* **2004**; 25: 3717-23. doi: 10.1016/j.biomaterials.2003.10.055.
16. Boroumand S, Haeri A, Nazeri N, Rabbani S. Review insights in cardiac tissue engineering: cells, scaffolds, and pharmacological agents. *Iran J Pharm Res* **2021**; 20: 467-96. doi: 10.22037/ijpr.2021.114730.15012.
17. González-González AM, Cruz R, Rosales-Ibáñez R, Hernández-Sánchez F, Carrillo-Escalante HJ, Rodríguez-Martínez JJ, et al. In vitro and in vivo evaluation of a polycaprolactone (PCL)/polylactic-co-glycolic acid (PLGA) (80:20) scaffold for improved treatment of chondral (cartilage) injuries. *Polymers (Basel)* **2023**; 15: 2324. doi: 10.3390/polym15102324.
18. Ma Z, He W, Yong T, Ramakrishna S. Grafting of gelatin on electrospun poly(caprolactone) nanofibers to improve endothelial cell spreading and proliferation and to control cell Orientation. *Tissue Eng* **2005**; 11: 1149-58. doi: 10.1089/ten.2005.11.1149.
19. Rodríguez-Martín M, Aguilar JM, Castro-Criado D, Romero A. Characterization of gelatin-polycaprolactone membranes by electrospinning. *Biomimetics (Basel)* **2024**; 9: 70. doi: 10.3390/biomimetics9020070.
20. El-Seedi HR, Said NS, Yosri N, Hawash HB, El-Sherif DM, Abouzid M, et al. Gelatin nanofibers: Recent insights in synthesis, bio-medical applications and limitations. *Heliyon* **2023**; 9: e16228. doi: 10.1016/j.heliyon.2023.e16228.
21. Chong EJ, Phan TT, Lim IJ, Zhang YZ, Bay BH, Ramakrishna S, et al. Evaluation of electrospun PCL/gelatin nanofibrous scaffold for wound healing and layered dermal reconstitution. *Acta Biomater* **2007**; 3: 321-30. doi: 10.1016/j.actbio.2007.01.002.
22. Kitsara M, Agbulut O, Kontziampasis D, Chen Y, Menasché P. Fibers for hearts: a critical review on electrospinning for cardiac tissue engineering. *Acta Biomater* **2017**; 48: 20-40. doi: 10.1016/j.actbio.2016.11.014.
23. Gnani S, di Blasio L, Tonda-Turo C, Mancardi A, Primo L, Ciardelli G, et al. Gelatin-based hydrogel for vascular endothelial growth factor release in peripheral nerve tissue engineering. *J Tissue Eng Regen Med* **2017**; 11: 459-70. doi: 10.1002/term.1936.
24. Kazemi Asl S, Rahimzadegan M, Kazemi Asl A. Progress in cardiac tissue engineering and regeneration: Implications of gelatin-based hybrid scaffolds. *Int J Biol Macromol* **2024**; 261: 129924. doi: 10.1016/j.ijbiomac.2024.129924.
25. Babitha S, Rachita L, Karthikeyan K, Shoba E, Janani I, Poornima B, et al. Electrospun protein nanofibers in healthcare: a review. *Int J Pharm* **2017**; 523: 52-90. doi: 10.1016/j.ijpharm.2017.03.013.
26. Nagiah N, El Khoury R, Othman MH, Akimoto J, Ito Y, Roberson DA, et al. Development and characterization of furfuryl-gelatin electrospun scaffolds for cardiac tissue engineering. *ACS Omega* **2022**; 7: 13894-905. doi: 10.1021/acsomega.2c00271.
27. Elamparathi A, Punnoose AM, Paul SF, Kuruvilla S. Gelatin electrospun nanofibrous matrices for cardiac tissue engineering applications. *Int J Polym Mater Polym Biomater* **2017**; 66: 20-7. doi: 10.1080/00914037.2016.1180616.
28. Doudi S, Barzegar M, Angouraj Taghavi E, Eini M, Ehterami A, Stokes K, et al. Applications of acellular human amniotic membrane in regenerative medicine. *Life Sci* **2022**; 310: 121032. doi: 10.1016/j.lfs.2022.121032.
29. Gautam S, Sharma C, Purohit SD, Singh H, Dinda AK, Potdar PD, et al. Gelatin-polycaprolactone-nanohydroxyapatite electrospun nanocomposite scaffold for bone tissue engineering. *Mater Sci Eng C Mater Biol Appl* **2021**; 119: 111588. doi: 10.1016/j.msec.2020.111588.
30. Ghasemi-Mobarakeh L, Prabhakaran MP, Morshed M, Nasr-Esfahani MH, Ramakrishna S. Electrospun poly(epsilon-caprolactone)/gelatin nanofibrous scaffolds for nerve tissue engineering. *Biomaterials* **2008**; 29: 4532-9. doi: 10.1016/j.biomaterials.2008.08.007.
31. Farzamfar S, Aleahmad M, Savari Kouzehkonan G, Salehi M, Nazeri N. Polycaprolactone/gelatin nanofibrous scaffolds for tissue engineering. *Biointerface Res Appl Chem* **2020**; 11: 11104-15. doi: 10.33263/briac114.111041115.
32. Peng W, Ren S, Zhang Y, Fan R, Zhou Y, Li L, et al. MgO nanoparticles-incorporated PCL/gelatin-derived coaxial electrospinning nanocellulose membranes for periodontal tissue regeneration. *Front Bioeng Biotechnol* **2021**; 9: 668428. doi: 10.3389/fbioe.2021.668428.
33. Semitela Â, Girão AF, Fernandes C, Ramalho G, Bdikin I, Completo A, et al. Electrospinning of bioactive polycaprolactone-gelatin nanofibres with increased pore size for cartilage tissue engineering applications. *J Biomater Appl* **2020**; 35: 471-84. doi: 10.1177/0885328220940194.
34. Darshan TG, Chen CH, Kuo CY, Shalumon KT, Chien YM, Kao HH, et al. Development of high resilience spiral wound suture-embedded gelatin/PCL/heparin nanofiber membrane scaffolds for tendon tissue engineering. *Int J Biol Macromol* **2022**; 221: 314-33. doi: 10.1016/j.ijbiomac.2022.09.001.
35. Gil-Castell O, Badia JD, Ontoria-Oviedo I, Castellano D, Sepúlveda P, Ribes-Greus A. Polycaprolactone/gelatin-based scaffolds with tailored performance: in vitro and in vivo validation. *Mater Sci Eng C Mater Biol Appl* **2020**; 107: 110296. doi: 10.1016/j.msec.2019.110296.
36. Kai D, Prabhakaran MP, Jin G, Ramakrishna S. Guided orientation of cardiomyocytes on electrospun aligned nanofibers for cardiac tissue engineering. *J Biomed Mater Res B Appl Biomater* **2011**; 98: 379-86. doi: 10.1002/jbm.b.31862.
37. Suh DY, Boden SD, Louis-Ugbo J, Mayr M, Murakami H, Kim HS, et al. Delivery of recombinant human bone morphogenetic protein-2 using a compression-resistant matrix in posterolateral spine fusion in the rabbit and in the non-human primate. *Spine (Phila Pa 1976)* **2002**; 27: 353-60. doi: 10.1097/00007632-200202150-00006.

38. Liu B, Lun DX. Current application of β -tricalcium phosphate composites in orthopaedics. *Orthop Surg* **2012**; 4: 139-44. doi: 10.1111/j.1757-7861.2012.00189.x.
39. Moccia F, Negri S, Shekha M, Faris P, Guerra G. Endothelial Ca²⁺ signaling, angiogenesis and vasculogenesis: just what it takes to make a blood vessel. *Int J Mol Sci* **2019**; 20: 3962. doi: 10.3390/ijms20163962.
40. Fearnley CJ, Roderick HL, Bootman MD. Calcium signaling in cardiac myocytes. *Cold Spring Harb Perspect Biol* **2011**; 3: a004242. doi: 10.1101/cshperspect.a004242.
41. Ye X, Zhang Y, Liu T, Chen Z, Chen W, Wu Z, et al. Beta-tricalcium phosphate enhanced mechanical and biological properties of 3D-printed polyhydroxyalkanoates scaffold for bone tissue engineering. *Int J Biol Macromol* **2022**; 209: 1553-61. doi: 10.1016/j.ijbiomac.2022.04.056.
42. Zhang Y, Wu D, Zhao X, Pakvasa M, Tucker AB, Luo H, et al. Stem cell-friendly scaffold biomaterials: applications for bone tissue engineering and regenerative medicine. *Front Bioeng Biotechnol* **2020**; 8: 598607. doi: 10.3389/fbioe.2020.598607.
43. Van der Schueren L, De Schoenmaker B, Kalaoglu ÖI, De Clerck K. An alternative solvent system for the steady state electrospinning of polycaprolactone. *Eur Polym J* **2011**; 47: 1256-63. doi: 10.1016/j.eurpolymj.2011.02.025.
44. Zhu B, Li W, Chi N, Lewis RV, Osamor J, Wang R. Optimization of glutaraldehyde vapor treatment for electrospun collagen/silk tissue engineering scaffolds. *ACS Omega* **2017**; 2: 2439-50. doi: 10.1021/acsomega.7b00290.
45. Tamimi M, Rajabi S, Pezeshki-Modaress M. Cardiac ECM/chitosan/alginate ternary scaffolds for cardiac tissue engineering application. *Int J Biol Macromol* **2020**; 164: 389-402. doi: 10.1016/j.ijbiomac.2020.07.134.
46. Bunaciu AA, Udriștiou EG, Aboul-Enein HY. X-ray diffraction: instrumentation and applications. *Crit Rev Anal Chem* **2015**; 45: 289-99. doi: 10.1080/10408347.2014.949616.
47. Smith BC. *Fundamentals of Fourier Transform Infrared Spectroscopy*. CRC Press; **2011**. doi: 10.1201/b10777.
48. Rezvani Ghomi E, Chellappan V, Esmayeli Neisany R, Dubey N, Amuthavalli K, Verma NK, et al. An innovative tunable bimodal porous PCL/gelatin dressing fabricated by electrospinning and 3D printing for efficient wound healing and scalable production. *Compos Sci Technol* **2024**; 247: 110402. doi: 10.1016/j.compscitech.2023.110402.
49. Zamani S, Salehi M, Ehterami A, Fauzi MB, Abbaszadeh-Goudarzi G. Assessing the efficacy of curcumin-loaded alginate hydrogel on skin wound healing: a gene expression analysis. *J Biomater Appl* **2024**; 38: 957-74. doi: 10.1177/08853282241238581.
50. Rezaie Kolarjani N, Mirzaii M, Zamani S, Maghsoodifar H, Naeiji M, Douki S, et al. Assessment of the ability of *Pseudomonas aeruginosa* and *Staphylococcus aureus* to create biofilms during wound healing in a rat model treated with carboxymethyl cellulose/carboxymethyl chitosan hydrogel containing EDTA. *Int Wound J* **2024**; 21: e14878. doi: 10.1111/iwj.14878.
51. Baheiraei N, Yeganeh H, Ai J, Gharibi R, Ebrahimi-Barough S, Azami M, et al. Preparation of a porous conductive scaffold from aniline pentamer-modified polyurethane/PCL blend for cardiac tissue engineering. *J Biomed Mater Res A* **2015**; 103: 3179-87. doi: 10.1002/jbm.a.35447.
52. Ghasemi M, Turnbull T, Sebastian S, Kempson I. The MTT assay: utility, limitations, pitfalls, and interpretation in bulk and single-cell analysis. *Int J Mol Sci* **2021**; 22: 12827. doi: 10.3390/ijms222312827.
53. Mehrabi A, Baheiraei N, Adabi M, Amirkhani Z. Development of a novel electroactive cardiac patch based on carbon nanofibers and gelatin encouraging vascularization. *Appl Biochem Biotechnol* **2020**; 190: 931-48. doi: 10.1007/s12010-019-03135-6.
54. Ahuja R, Kumari N, Srivastava A, Bhati P, Vashisth P, Yadav PK, et al. Biocompatibility analysis of PLA based candidate materials for cardiovascular stents in a rat subcutaneous implant model. *Acta Histochem* **2020**; 122: 151615. doi: 10.1016/j.acthis.2020.151615.
55. Roacho-Pérez JA, Garza-Treviño EN, Moncada-Saucedo NK, Carriquiry-Chequer PA, Valencia-Gómez LE, Matthews ER, et al. Artificial scaffolds in cardiac tissue engineering. *Life (Basel)* **2022**; 12: 1117. doi: 10.3390/life12081117.
56. Payan SM, Hubert F, Rochais F. Cardiomyocyte proliferation, a target for cardiac regeneration. *Biochim Biophys Acta Mol Cell Res* **2020**; 1867: 118461. doi: 10.1016/j.bbamcr.2019.03.008.
57. Ponnusamy M, Liu F, Zhang YH, Li RB, Zhai M, Liu F, et al. Long noncoding RNA CPR (cardiomyocyte proliferation regulator) regulates cardiomyocyte proliferation and cardiac repair. *Circulation* **2019**; 139: 2668-84. doi: 10.1161/circulationaha.118.035832.
58. Leone M, Magadum A, Engel FB. Cardiomyocyte proliferation in cardiac development and regeneration: a guide to methodologies and interpretations. *Am J Physiol Heart Circ Physiol* **2015**; 309: H1237-50. doi: 10.1152/ajpheart.00559.2015.
59. Wang F, Guan J. Cellular cardiomyoplasty and cardiac tissue engineering for myocardial therapy. *Adv Drug Deliv Rev* **2010**; 62: 784-97. doi: 10.1016/j.addr.2010.03.001.
60. Liao B, Zhang D, Bursac N. Functional cardiac tissue engineering. *Regen Med* **2012**; 7: 187-206. doi: 10.2217/rme.11.122.
61. Sampaio-Pinto V, Janssen J, Chirico N, Serra M, Alves PM, Doevendans PA, et al. A roadmap to cardiac tissue-engineered construct preservation: insights from cells, tissues, and organs. *Adv Mater* **2021**; 33: e2008517. doi: 10.1002/adma.202008517.
62. Turksen K. *Cell Biology and Translational Medicine*. Vol 4. Springer; **2018**.
63. Sridharan D, Palaniappan A, Blackstone BN, Dougherty JA, Kumar N, Seshagiri PB, et al. In situ differentiation of human-induced pluripotent stem cells into functional cardiomyocytes on a coaxial PCL-gelatin nanofibrous scaffold. *Mater Sci Eng C Mater Biol Appl* **2021**; 118: 111354. doi: 10.1016/j.msec.2020.111354.
64. Echeverria Molina MI, Malollari KG, Komvopoulos K. Design challenges in polymeric scaffolds for tissue engineering. *Front Bioeng Biotechnol* **2021**; 9: 617141. doi: 10.3389/fbioe.2021.617141.
65. Roacho-Pérez JA, Garza-Treviño EN, Moncada-Saucedo NK, Carriquiry-Chequer PA, Valencia-Gómez LE, Matthews ER, et al. Artificial scaffolds in cardiac tissue engineering. *Life (Basel)* **2022**; 12: 1117. doi: 10.3390/life12081117.
66. Balu R, Kumar TS, Ramalingam M, Ramakrishna S. Electrospun polycaprolactone/poly(1,4-butylene adipate-co-polycaprolactam) blends: potential biodegradable scaffold for bone tissue regeneration. *J Biomater Tissue Eng* **2011**; 1: 30-9. doi: 10.1166/jbtt.2011.1004.
67. Lu X, Zou H, Liao X, Xiong Y, Hu X, Cao J, et al. Construction of PCL-collagen@PCL@PCL-gelatin three-layer small diameter artificial vascular grafts by electrospinning. *Biomed Mater* **2022**; 18: 015008. doi: 10.1088/1748-605X/aca269.
68. Liu Q, Cen L, Yin S, Chen L, Liu G, Chang J, et al. A comparative study of proliferation and osteogenic differentiation of adipose-derived stem cells on akermanite and beta-TCP ceramics. *Biomaterials* **2008**; 29: 4792-9. doi: 10.1016/j.biomaterials.2008.08.039.
69. Yu S, Shi J, Liu Y, Si J, Yuan Y, Liu C. A mechanically robust and flexible PEGylated poly(glycerol sebacate)/ β -TCP nanoparticle composite membrane for guided bone regeneration. *J Mater Chem B* **2019**; 7: 3279-90. doi: 10.1039/c9tb00417c.
70. Sadri N, Rajabi M, Akbari B, Firouzi M, Hassannejad Z. Fabrication and characterization of gold nanoparticle-doped electrospun PCL/chitosan nanofibrous scaffolds for nerve tissue engineering. *J Mater Sci Mater Med* **2018**; 29: 134. doi: 10.1007/s10856-018-6144-3.
71. Roshanghias A, Sodeifian G, Javidparvar AA, Tarashi S. Construction of a novel polytetrafluoroethylene-based sealant paste: the effect of polyvinyl butyral (PVB) and nano-alumina on the sealing performance and construction formulations. *Results Eng* **2022**; 14: 100460. doi: 10.1016/j.rineng.2022.100460.
72. Jung MR, Horgen FD, Orski SV, Rodriguez CV, Beers KL, Balazs GH, et al. Validation of ATR FT-IR to identify polymers of plastic marine debris, including those ingested by marine

- organisms. *Mar Pollut Bull* **2018**; 127: 704-16. doi: 10.1016/j.marpolbul.2017.12.061.
73. Ki CS, Baek DH, Gang KD, Lee KH, Um IC, Park YH. Characterization of gelatin nanofiber prepared from gelatin-formic acid solution. *Polymer* **2005**; 46: 5094-102. doi: 10.1016/j.polymer.2005.04.040.
 74. Saket Bejandi M, Behrooz MH, Khalili MR, Sharifi R, Javidparvar AA, Oguzie E. Pharmaceuticals for materials protection: experimental and computational studies of expired closantel drug (C₂₂H₁₄Cl₂I₂N₂O₂) as a potent corrosion inhibitor. *J Ind Eng Chem* **2024**; 131: 662-75. doi: 10.1016/j.jiec.2023.11.003.
 75. Nandiyanto AB, Oktiani R, Ragadhita R. How to read and interpret FTIR spectroscopy of organic material. *Indones J Sci Technol* **2019**; 4: 97-118. doi: 10.17509/ijost.v4i1.15806.
 76. Abd El-Hamid HK, Farag MM, Abdelraof M, Elwan RL. Regulation of the antibiotic elution profile from tricalcium phosphate bone cement by addition of bioactive glass. *Sci Rep* **2024**; 14: 2804. doi: 10.1038/s41598-024-53319-2.
 77. Wang W, Zhou X, Wang H, Zhou G, Yu X. Fabrication and evaluation of PCL/PLGA/ β -TCP spiral-structured scaffolds for bone tissue engineering. *Bioengineering (Basel)* **2024**; 11: 732. doi: 10.3390/bioengineering11070732.
 78. Krobot Š, Melčová V, Menčík P, Kontárová S, Rampichová M, Hedvičáková V, et al. Poly(3-hydroxybutyrate) (PHB) and polycaprolactone (PCL) based blends for tissue engineering and bone medical applications processed by FDM 3D printing. *Polymers (Basel)* **2023**; 15: 2404. doi: 10.3390/polym15102404.
 79. Wang X, Xiang L, Peng Y, Dai Z, Hu Y, Pan X, et al. Gelatin/polycaprolactone electrospun nanofibrous membranes: the effect of composition and physicochemical properties on postoperative cardiac adhesion. *Front Bioeng Biotechnol* **2021**; 9: 792893. doi: 10.3389/fbioe.2021.792893.
 80. Engelmayer GC Jr, Cheng M, Bettinger CJ, Borenstein JT, Langer R, Freed LE. Accordion-like honeycombs for tissue engineering of cardiac anisotropy. *Nat Mater* **2008**; 7: 1003-10. doi: 10.1038/nmat2316.
 81. Fan L, Yang H, Yang J, Peng M, Hu J. Preparation and characterization of chitosan/gelatin/PVA hydrogel for wound dressings. *Carbohydr Polym* **2016**; 146: 427-34. doi: 10.1016/j.carbpol.2016.03.002.
 82. Zamani S, Rezaei Kolarijani N, Naeiji M, Vaez A, Maghsoodifar H, Sadeghi Douki SA, et al. Development of carboxymethyl cellulose/gelatin hydrogel loaded with omega-3 for skin regeneration. *J Biomater Appl* **2024**; 39: 377-95. doi: 10.1177/08853282241265769.
 83. Fan S, Wu X, Fang Z, Yang G, Yang J, Zhong W, et al. Injectable and ultra-compressible shape-memory mushroom: highly aligned microtubules for ultra-fast blood absorption and hemostasis. *Chem Eng J* **2023**; 460: 140554. doi: 10.1016/j.cej.2022.140554.
 84. Yang Y, Liang Y, Chen J, Duan X, Guo B. Mussel-inspired adhesive antioxidant antibacterial hemostatic composite hydrogel wound dressing via photo-polymerization for infected skin wound healing. *Bioact Mater* **2022**; 8: 341-54. doi: 10.1016/j.bioactmat.2021.06.014.
 85. Stavropoulos A, Windisch P, Szendrői-Kiss D, Peter R, Gera I, Sculean A. Clinical and histologic evaluation of granular Beta-tricalcium phosphate for the treatment of human intrabony periodontal defects: a report on five cases. *J Periodontol* **2010**; 81: 325-34. doi: 10.1902/jop.2009.090386.
 86. Kitsara M, Revet G, Vartanian-Grimaldi JS, Simon A, Minguy M, Miche A, et al. Cyto- and bio-compatibility assessment of plasma-treated polyvinylidene fluoride scaffolds for cardiac tissue engineering. *Front Bioeng Biotechnol* **2022**; 10: 1008436. doi: 10.3389/fbioe.2022.1008436.
 87. Baheiraei N, Nourani MR, Mortazavi SM, Movahedin M, Eyni H, Bagheri F, et al. Development of a bioactive porous collagen/ β -tricalcium phosphate bone graft assisting rapid vascularization for bone tissue engineering applications. *J Biomed Mater Res A* **2018**; 106: 73-85. doi: 10.1002/jbm.a.36207.
 88. Park HJ, Min KD, Lee MC, Kim SH, Lee OJ, Ju HW, et al. Fabrication of 3D porous SF/ β -TCP hybrid scaffolds for bone tissue reconstruction. *J Biomed Mater Res A* **2016**; 104: 1779-87. doi: 10.1002/jbm.a.35711.
 89. Ghaedamini S, Karbasi S, Hashemibeni B, Honarvar A, Rabiei A. PCL/agarose 3D-printed scaffold for tissue engineering applications: fabrication, characterization, and cellular activities. *Res Pharm Sci* **2023**; 18: 566-79. doi: 10.4103/1735-5362.383711.
 90. Chen X, Feng B, Zhu DQ, Chen YW, Ji W, Ji TJ, et al. Characteristics and toxicity assessment of electrospun gelatin/PCL nanofibrous scaffold loaded with graphene in vitro and in vivo. *Int J Nanomedicine* **2019**; 14: 3669-78. doi: 10.2147/ijn.S204971.
 91. Broadway-Stringer S, Jiang H, Wadmore K, Hooper C, Douglas G, Steeples V, et al. Insights into the role of a cardiomyopathy-causing genetic variant in ACTN2. *Cells* **2023**; 12: 721. doi: 10.3390/cells12050721.
 92. Michela P, Velia V, Aldo P, Ada P. Role of connexin 43 in cardiovascular diseases. *Eur J Pharmacol* **2015**; 768: 71-6. doi: 10.1016/j.ejphar.2015.10.030.
 93. Zu L, Wen N, Liu C, Zhao M, Zheng L. Connexin43 and myocardial ischemia-reperfusion injury. *Cardiovasc Hematol Disord Drug Targets* **2018**; 18: 14-6. doi: 10.2174/1871529x16666161227143644.
 94. Kajioka S, Takahashi-Yanaga F, Shahab N, Onimaru M, Matsuda M, Takahashi R, et al. Endogenous cardiac troponin T modulates Ca²⁺-mediated smooth muscle contraction. *Sci Rep* **2012**; 2: 979. doi: 10.1038/srep00979.
 95. Yang G, Mahadik B, Choi JY, Fisher JP. Vascularization in tissue engineering: fundamentals and state-of-art. *Prog Biomed Eng (Bristol)* **2020**; 2: 012002. doi: 10.1088/2516-1091/ab5637.
 96. Xiao X, Wang W, Liu D, Zhang H, Gao P, Geng L, et al. The promotion of angiogenesis induced by three-dimensional porous beta-tricalcium phosphate scaffold with different interconnection sizes via activation of PI3K/Akt pathways. *Sci Rep* **2015**; 5: 9409. doi: 10.1038/srep09409.
 97. Moradi N, Kaviani S, Soufizomorrod M, Hosseinzadeh S, Soleimani M. Preparation of poly(acrylic acid)/tricalcium phosphate nanoparticles scaffold: characterization and releasing UC-MSCs derived exosomes for bone differentiation. *Bioimpacts* **2023**; 13: 425-38. doi: 10.34172/bi.2022.24142.
 98. Teymori M, Karimi E, Saburi E. Evaluation of osteoconductive effect of polycaprolactone (PCL) scaffold treated with *Aloe vera* on adipose-derived mesenchymal stem cells (ADSCs). *Am J Stem Cells* **2023**; 12: 83-91.
 99. Bohner M, Santoni BLG, Döbelin N. β -tricalcium phosphate for bone substitution: synthesis and properties. *Acta Biomater* **2020**; 113: 23-41. doi: 10.1016/j.actbio.2020.06.022.
 100. Takahashi H, Shibuya M. The vascular endothelial growth factor (VEGF)/VEGF receptor system and its role under physiological and pathological conditions. *Clin Sci (Lond)* **2005**; 109: 227-41. doi: 10.1042/cs20040370.
 101. Umapathy A, Chamley LW, James JL. Reconciling the distinct roles of angiogenic/anti-angiogenic factors in the placenta and maternal circulation of normal and pathological pregnancies. *Angiogenesis* **2020**; 23: 105-17. doi: 10.1007/s10456-019-09694-w.
 102. Moradi N, Soufi-Zomorrod M, Hosseinzadeh S, Soleimani M. Poly(acrylic acid)/tricalcium phosphate nanoparticles scaffold enriched with exosomes for cell-free therapy in bone tissue engineering: an in vivo evaluation. *Bioimpacts* **2024**; 14: 27510. doi: 10.34172/bi.2023.27510.
 103. Bellen F, Carbone E, Baatsen P, Jones EAV, Kabirian F, Heying R. Improvement of endothelial cell-polycaprolactone interaction through surface modification via aminolysis, hydrolysis, and a combined approach. *J Tissue Eng Regen Med* **2023**; 2023: 5590725. doi: 10.1155/2023/5590725.
 104. Wang X, Lin M, Kang Y. Engineering porous β -tricalcium phosphate (β -TCP) scaffolds with multiple channels to promote cell migration, proliferation, and angiogenesis. *ACS Appl Mater Interfaces* **2019**; 11: 9223-32. doi: 10.1021/acsami.8b22041.
 105. Hall C, Gehmlich K, Denning C, Pavlovic D. Complex relationship

- between cardiac fibroblasts and cardiomyocytes in health and disease. *J Am Heart Assoc* **2021**; 10: e019338. doi: 10.1161/jaha.120.019338.
106. Di Baldassarre A, Cimetta E, Bollini S, Gaggi G, Ghinassi B. Human-induced pluripotent stem cell technology and cardiomyocyte generation: progress and clinical applications. *Cells* **2018**; 7: 48. doi: 10.3390/cells7060048.
 107. Lee S, Serpooshan V, Tong X, Venkatraman S, Lee M, Lee J, et al. Contractile force generation by 3D hiPSC-derived cardiac tissues is enhanced by rapid establishment of cellular interconnection in matrix with muscle-mimicking stiffness. *Biomaterials* **2017**; 131: 111-20. doi: 10.1016/j.biomaterials.2017.03.039.
 108. Ferri JM, Gisbert I, García-Sanoguera D, Reig MJ, Balart R. The effect of beta-tricalcium phosphate on mechanical and thermal performances of poly(lactic acid). *J Compos Mater*. **2016**; 50: 4189-98. doi: 10.1177/0021998316636205.
 109. Tovar N, Shen C, Wang M, Witek L, Cronstein B, Torroni A, et al. Transforming the degradation rate of β -tricalcium phosphate bone replacement using 3D printers. *J Oral Maxillofac Surg* **2021**; 79: e56. doi: 10.1016/j.joms.2021.08.079.
 110. Cui Z, Zhang Y, Cheng Y, Gong D, Wang W. Microstructure, mechanical, corrosion properties and cytotoxicity of beta-calcium polyphosphate reinforced ZK61 magnesium alloy composite by spark plasma sintering. *Mater Sci Eng C Mater Biol Appl* **2019**; 99: 1035-47. doi: 10.1016/j.msec.2019.02.050.
 111. Pan C, Sun X, Xu G, Su Y, Liu D. The effects of β -TCP on mechanical properties, corrosion behavior and biocompatibility of β -TCP/Zn-Mg composites. *Mater Sci Eng C Mater Biol Appl* **2020**; 108: 110397. doi: 10.1016/j.msec.2019.110397.
 112. Liu B, Lun DX. Current application of β -tricalcium phosphate composites in orthopaedics. *Orthop Surg* **2012**; 4: 139-44. doi: 10.1111/j.1757-7861.2012.00189.x.
 113. Murayama A, Ajiki T, Hayashi Y, Takeshita K. A unidirectional porous beta-tricalcium phosphate promotes angiogenesis in a vascularized pedicle rat model. *J Orthop Sci* **2019**; 24: 1118-24. doi: 10.1016/j.jos.2019.07.015.
 114. Wang X, Wang L, Wu Q, Bao F, Yang H, Qiu X, et al. Chitosan/calcium silicate cardiac patch stimulates cardiomyocyte activity and myocardial performance after infarction by synergistic effect of bioactive ions and aligned nanostructure. *ACS Appl Mater Interfaces* **2019**; 11: 1449-68. doi: 10.1021/acsami.8b17754.